Title

ON DEFINING THE TURBULENT BURNING VELOCITY IN PREMIXED V-SHAPED TURBULENT FLAMES

Authors

Cheng, R.K.
Ng, T.T.

Publication Date

1984-03-01

LBL-17564
Preprint

Lawrence Berkeley Laboratory
UNIVERSITY OF CALIFORNIA

APPLIED SCIENCE DIVISION

Submitted to Combustion and Flame

ON DEFINING THE TURBULENT BURNING VELOCITY IN PREMIXED V-SHAPED TURBULENT FLAMES

R.K. Cheng and T.T. Ng

March 1984

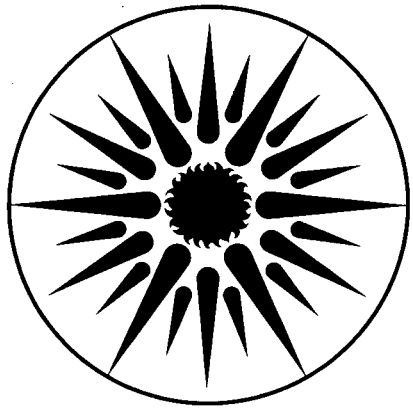

APPLIED SCIENCE DIVISION

Prepared for the U.S. Department of Energy under Contract DE-AC03-76SF00098

DISCLAIMER

On Defining the Turbulent Burning Velocity in Premixed V-Shaped Turbulent Flames

R. K. Cheng and T. T. Ng

Applied Science Division
Lawrence Berkeley Laboratory
University of California
Berkeley, Ca 94720

ABSTRACT

Turbulent burning velocity S_t, is determined for six premixed v-shaped turbulent flames. In addition to defining S_t with respect to the conventional flame surface, a definition based on an effective flame orientation is proposed. The results based on the flame surface increase significantly with distance from the flame stabilizer. In general, they compare quite poorly with experimental correlation obtained by others. However, the results based on the effective flame orientation are more consistent and provide better comparison. These results indicate that the flame surface method is not a consistent method for deducing the turbulent burning velocity in this flame configuration.

INTRODUCTION

The increase in propagation velocity of premixed flame due to fluid mechanical turbulence can be expressed by a turbulent burning velocity, S_t, by analogy with the laminar burning velocity, S_u. Whereas the laminar burning velocity is a unique property for a given state and reactant composition, the turbulent burning velocity is affected by the properties of the incident turbulence, and perhaps burner geometry. Despite a large number of experimental and theoretical studies of turbulent flames, the detailed mechanisms responsible for the increase in burning velocity are not yet fully understood and characterized.

Turbulent burning velocity is important intermediary to link the parameters of turbulence with chemical kinetics. It is often used for comparing experimental measurements and theoretical calculations [1-3]. The basic concept of turbulent burning velocity associates the increase in flame velocity with the scale and intensity of the incident turbulence. For a fixed state and reactant composition, the ratio of turbulent burning velocity to laminar burning velocity (S_t / S_u) should be proportional to the properties of the incident turbulence. Therefore, S_t data are usually correlated with empirical turbulence parameters. Ballal & Lefebvre [4] correlated (S_t / S_u) with the integral length scale, l_x, of the incident turbulence. Abdel-Gayed and Bradley [5] report an extensive survey of the turbulent burning velocities obtained in many different experimental apparatus covering a wide range of initial conditions, mixtures and turbulence intensities. They propose correlating (S_t / S_u) at a given turbulent Reynolds number , $R_l = u' l_x / \nu$, with the ratio of the laminar burning velocity to the root-mean-square (RMS) velocity of the incident turbulence fluctuations (S_u / u').

Experimental determination of the turbulent burning velocity usually requires defining a flame surface to represent the thick turbulent flame brush, in addition to measuring the mean velocity entering the flame. In the past, flow visualization has been the only convenient means to infer the flame surface, even though the technique is not highly accurate. With the use of more advanced diagnostics, consistent and reproducible flame surface can be established from time and space resolved scalar or

velocity data within the turbulent flame.

The objective of this paper is to determine the turbulent burning velocities in ethylene/air v-shaped turbulent flames using velocity statistical data obtained by laser Doppler velocimetry (LDV). Details of mean velocities, root-mean-square (RMS) fluctuations, and Reynolds stress we have measured within the flame have been reported in our earlier papers [6,7]. The experimental conditions cover free-stream velocity U_∞ from 5.0 to 7.0 m/s, ethylene/air equivalence ratio, φ, from 0.66 to 0.8 and incident turbulence intensities from 5 to 8 %. Under these experimental conditions, the turbulent flame can be classified as a wrinkled laminar flame. Two-point density measurements [8] have shown that the turbulent flame consists of a continuous fluctuating thin flame sheet. As discussed in [7], the significant increase in turbulent intensities and Reynolds stress within the flame region appear to be the effects of intermittent velocity measurement in the burned and the unburned states.

Measurements of the turbulent burning velocity in v-shaped flames have been reported by Ho et.al. [9], Smith and Gouldin [10], and Dandekar and Gouldin [11]. Ho et.al. [9] define the flame surface of a stoichiometric methane/air flame using temperature data obtained with rhodium hot wire. They estimate the turbulent burning velocity of this flame to be the normal component of the free-stream velocity with respect to the flame surface. Smith and Gouldin [10] determine the flame surface for their methane/air flames with thermocouples, and measure the approach flow velocitywith hot-wire and LDV. Their turbulent burning velocity data are correlated with both the macroscale Reynolds number (R_l) and the microscale Reynolds number (R_λ). Subsequent work of Dandekar and Gouldin [11] involves measurement of turbulent burning velocity in methane/air, propane/air and ethylene/air flames. They question whether or not the length scales and fluctuating velocities of the incident turbulence are sufficient to correlate the turbulent burning velocity.

All of the previous experimental measurements [9-11] are concerned with determining S_t for a fixed location above the flame stabilizer. As shown in our previous work [7], the properties of the turbulent flame change along the flame brush. Since our

velocity data cover the entire flow field, local S_t's are determined for various positions above the flame stabilizer. As shall be seen later, these local turbulent burning velocities also vary along the flame brush. This shows that to obtain a representative S_t for the v-shaped flames, measurement at a single point may not be sufficient.

Two methods are used to deduce S_t. The first is the conventional method of defining S_t with reference to a flame surface. This flame surface represents the overall geometry of the flame brush. The second method, which we have developed, is based on an effective flame orientation. The effective flame orientation is shown to be more consistent with the geometry of the flame convolutions. It is based on the deflection of the velocity through the flame brush. The second method, which can be obtained conveniently from our data, is proposed as an alternate means to deduce S_t because the use of the first method produces results which are inconsistent and sometimes non-physical.

In laminar flame, the two methods are identical because the flame surface coincides with the effective flame orientation. In turbulent flames, the two methods should produce similar results if a consistent "universal" turbulent burning velocity exists. However, as shall be seen later, S_t's based on the two methods are quite different. This difference emphasizes the need to standardize the method for defining the turbulent burning velocity in this flame configuration. Otherwise, the results would not be useful for the development of numerical model for turbulent combustion.

EXPERIMENTAL SYSTEM

Fig. 1 shows a schematic of the experimental system. The v-shaped flame is stabilized by a 1.0 mm rod in a unconfined circular co-axial jet with an inner core of ethylene/air mixture 5.0 cm in diameter surrounded by an outer annular jet of air 10.0 cm in diameter. The function of the outer jet is to shield the fuel/air jet from the mixing layer formed with the room air. The turbulence generator is placed 5.0 cm upstream. The center of the turbulence generator is the origin of the co-ordinate system, with the optical axis of the LDV system and the flame stabilizer rod parallel to the z axis. Velocity measurements are made on the x-y plane at the center. The

measurement grid consists of four to six axial (x) profiles at 10 cm or 5 cm intervals above the flame stabilizer, and thirty transverse (y) measurement points from the flame center to y = 30 mm. Details of the LDV system, the computer-controlled data acquisition system, and the data reduction methods are described in Ref. [6].

The mixture compositions and properties of the incident turbulence for the six experiments (labeled Flame #1 to #6) are listed in Table I. Also listed are the dimensions of the three turbulence generators. These mixture and turbulence parameters of our experiments correspond to (S_u/u') of 0.9 to 2.4 and R_l of 80 to 140. Therefore our turbulent flames are mostly within the wrinkled laminar flame regime of $S_u/u'>1$ prescribed by Abdel-Gayed and Bradley [5].

The turbulence intensity across the jet is found to be uniform and decays downstream from the generator. With U_∞ = 7.0 m/s,the incident turbulence decays from 5 % at x = 60 mm to 3.5% at x = 120 mm. With the presence of the flame, the incident turbulence decays more slowly due to additional turbulence generated by the fluctuating flame [9]. For Flame #3 through #6, the additional turbulence compensates the normal turbulence decay such that no significant reduction in the incident turbulence is observed. Ideally the turbulent burning velocity for these flames should be independent of position while the results for Flame #1 and #2 should show some decrease with positions downstream.

DETERMINATION OF TURBULENT BURNING VELOCITY

Method I : Time-Mean Flame Surface

The mean flame surface methods used for determining S_T all stem from similar techniques used for determining S_u. Among the criteria used for defining this surface are the most luminous contour, the cold boundary, the geometric center of the flame brush or the brightest (or darkest) contour shown on schlieren records. In laminar flames, these surfaces are parallel to each other because the laminar flame thickness is typically about 1.0 mm. However, in turbulent flames, the flame brush thickness increases to several times the laminar flame thickness, and these flame surfaces may

not be parallel, depending on the flame geometry.

In unstabilized turbulent flames, such as the expanding flame kernel, all the flame surfaces are parallel, and the flame propagates normal to the incident flow. The results would be the same regardless of which flame surface is used. In stabilized oblique flames, such as the one considers here, the flame surfaces are divergent due to the increase in flame brush thickness away from the flame stabilizer. Since the turbulent burning velocity is defined as the normal component of the incident velocity with respect to a chosen flame surface, the results would be different depending on which flame surface is used. For example, in Fig. 2, S_t deduced with respect to the cold boundary, as in Dandekar and Gouldin [11] would be larger than the S_t deduced with respect to the mean flame surface, as in Ho et.al. [9] and Smith and Gouldin [10].

In this study, the steepest gradient contour is chosen because this surface is consistent with the one used in most experimental studies. It is deduced from our velocity data by fitting parabolically the positions of maximum velocity gradient along the flame brush. These positions also represent the peak RMS velocity fluctuation points. Previous study [12] has also shown that the maximum density gradient and the maximum density fluctuation also occur close to these positions. Therefore this contour should be identical to the mean flame surface used by Ho et. al. [9] and to the mean schlieren surface used by Smith and Gouldin [10].

As depicted in Fig. 3, the turbulent burning velocity is therefore

$$S_t = U_1 \sin(\alpha - \vartheta_1) \tag{1}$$

where, α, is the local orientation of the mean flame surface or the local slope of the contour and ϑ_1 is the deflection of the velocity vector entering the flame brush, U_1. The velocity at the cold boundary of the flame region is used as U_1. The cold boundary of the flame region is defined as the position where the Reynolds stress shows an initial rise from its free-stream level [6].

Method II : Effective Flame Surface

The most apparent feature of the flow field as shown on Fig. 2 is the deflection of the flow from outward away from the flame center to inward across the flame brush. Although the changes in direction and magnitude of the mean vectors are quite gradual, particle tracking records [13] of seed particles traversing the convoluted thin flame sheet show quite abrupt changes.

The abrupt change in flow direction can be explain by a model of the local flame-flow interaction depicted in Fig. 4 (a). As in a planar oblique laminar flame, through this oblique flame sheet, only the velocity component orthogonal to the local instantaneous flame front is accelerated while the tangential component remains relatively unchanged. This causes the flow in the burned state to deflect inwards. The tangential velocity indicates that the flame segment is convected downstream. The convection is shown on our schlieren movies and has been discussed by others [14].

Since the flame sheet is convoluted, the orientation of the local instantaneous flame fronts are quite random. Suzuki et. al [15] have carried out a study of the movement of the local instantaneous flame front using two ion-probe technique. They also show that the direction of the flame front movement is normal to the orientation of the flame. Therefore, the most probable flame movement direction they have obtained also specifies a most probable flame front orientation. It is interesting to note that their results show that the most probable flame front orientation is quite different from the flame surfaces.

Since the conserved tangential velocity criterion prescribes a consistent relationship between the flow deflection and the flame orientation, this implies that the flame orientation can be deduced from the velocity data. Although the flame-flow interaction model is valid only at the local flame front, statistically, the net effect of all the interactions within the flame brush should produce the observed mean flow deflection. Therefore, the flow vectors entering and leaving the flame region, as in Fig. 4(b), can be use to determine an effective flame orientation. This orientation should be associated with the statistical mean of the most local probable flame orientations as shown by

results of Suzuki et. al. [15]. This effective flame orientation provides an alternative means of deducing the turbulent burning velocity.

According to this definition, S_t would be the velocity component of U_1 orthogonal to the effective flame orientation and is calculated from the following equations:

$$\tan \beta = \frac{U_1 \cos \vartheta_1 - U_2 \cos \vartheta_2}{U_1 \sin \vartheta_1 + U_2 \sin \vartheta_2} \tag{3}$$

$$S_t = U_1 \sin (\beta - \vartheta_1) \tag{4}$$

where β is the effective flame orientation angle with respect to the x-axis while ϑ_1 and ϑ_2 are the deflection of U_1 and U_2 respectively.

Ideally, the two velocity vectors should be selected by following the streamlines through the flame region. But due to combustion induced stream-tube divergence, it is not feasible to construct the streamlines. Therefore, the velocity vectors at the hot and cold boundaries at fixed axial location are used to calculate S_t. Since the velocity at the hot boundary are fairly independent of x, this procedure should be sufficient. It should be noted that this method is not applicable at $x \geq 70.0$ mm and throughout most part of a highly oblique flames where the burned region is influenced by the wake of the flame stabilizer.

RESULTS and DISCUSSIONS

Compared in Table II are the turbulent burning velocities for Flame #1 based on the mean flame surface $S_t(\alpha)$, and based on the effective flame orientation $S_t(\beta)$. The local values of α and β are also shown. The laminar burning velocity for the ethylene/air mixtures are obtained from Raezer and Olsen [16].

For the $S_t(\alpha)$'s, the most striking result is the negative value at x=60 mm. This indicate that the turbulent burning velocity is meaningless in this region close to the flame stabilizer where the wake of the stabilizer influence flame propagation. As shown on the schlieren movies, the flame sheet is ratively smooth and free of convolutions near x = 60.0mm. The development and growth of the flame convolutions occur further downstream. This suggests a lag time for the flame to fully react to the incident turbulence. In this configuration, the lag time is proportional to the distance

above the flame stabilizer. As Peterson and Emmons [14] have found that flame disturbances initiated by turbulence fluctuations at some frequencies are amplified while those at other frequencies are damped, this distance is expected to depend on the nature of the incident turbulence and also on the mixture composition. For our flames, the convolutions are reasonably well-developed at x ≥ 70.00 mm except for Flame #4 with lean fuel/air mixture where the flame convolutions only become apparent at x > 80.0 mm. Consequently, the results we have obtained near the flame stabilizer will not be discussed further and are not used for calculating the mean S_t.

Further downstream (x ≥ 70.0 mm), the $S_t(\alpha)$'s become positive and increase with increasing distance x. Also, all but one of the $S_t(\alpha)$'s are below the laminar burning velocity for this mixture. The increase of $S_t(\alpha)$'s with x is due to the increase in α as the flame region thickens and curves into the incident flow. This variation of S_t along conical turbulent flames has been reported by Kleine [17] and is discussed more recently in a review by Gunther [18]. If the variation is large, it would not be possible to deduce a representative mean value for comparison with different flames.

To compare our results directly with those obtained for ethylene by Dandekar and Gouldin [11], turbulent burning velocities for Flame #1 are deduced using their flame surface which is the cold boundary of the flame region. The results are shown in Table IIA. As to be expected, these turbulent burning velocities are higher than the $S_t(\alpha)$'s because α_{cb} is higher than α. Moreover, the results based on the cold boundary also increase with increasing distance x. Dandekar and Gouldin report measurement only at one location 25.0 mm from the stabilizer rod. For equivalence ratio of 0.7, with incident RMS turbulence fluctuation of 0.2 m/s, their S_t is about 0.8 m/s. The conditions of Flame #1 are very close to these conditions. At x = 80 mm (30 mm from the stabilizer) our data show S_t of 0.79 m/s. In view of the differences in the experimental systems and techniques, this comparison is indeed quite satisfactory. Dandekar and Gouldin also discuss that under similar incident turbulence level, the turbulent burning velocities for the ethylene flames are consistently lower than those for the methane and propane flames. This seem to indicate that their ethylene results are

somewhat lower than they have expected.

Although the use of the cold boundary gives results which are generally higher than the laminar burning velocity and may seem more physical, this does not seem to be a good rationale for choosing this surface. Both of the surfaces have been used and by far the majority of the published results have used, in one form or another, the steepest gradient contour. Questions regarding whether or not the two different surfaces would give consistent results have never been fully addressed. Moreover, the results based on the cold boundary are also non-uniform and spread over a larger range than the $S_t(\alpha)$'s. For example, in Table IIb, the result at x = 110 mm is almost four times higher than that at x = 60 mm. Therefore, using the cold boundary does not provide any improvement in obtaining a representative and consistent S_t for the turbulent flame.

In comparison, the $S_t(\beta)$'s are larger than the $S_t(\alpha)$'s and the $S_t(\alpha_{cb})$'s. The most interesting implications of the magnitude of β is that none of the flame surfaces, be it the steepest gradient contour or the cold boundary would be consistent with the overall deflection of the flow through the flame region. This is in accord with the experimental results of Suzuki et. al. [15] showing that the most probable flame orientations are much larger than the orientations prescribed by the flame boundaries.

It is interesting to note that the $S_t(\beta)$'s do not show an increase with distance x, though they scatter over a range comparable to that of the $S_t(\alpha)$'s, (Table II). For Flame #1 the $S_t(\beta)$'s average about 1.65m/s, which corresponds to S_t / S_u of 3.4. In comparison, the mean $S_t(\alpha)$'s is only 0.29 m/s, and the results based on the cold boundary average 0.94 m/s.

Shown in Fig. 5 are the profiles of the velocity components normal, U_n, and tangential, U_t, to the effective flame orientation at x = 90 mm for Flame #1. The velocities at y = 11.5 and 6.0 mm are used to calculate β. As can be seen, the U_n profile undergoes maximum increase and the changes in U_t is relatively minor. The increase in the normal velocities across the flame brush is by about a factor of 3.0, which is substantially lower than the inverse density ratio of about 7.0 for this composition. Mass

conservation normal to the effective flame orientation therefore suggests that the stream-tube divergence due to combustion heat release results in a cross-sectional area expansion of about 2.33. Using two-dimensional approximation, this area expansion ratio can be approximated by $(Sin(\beta-\vartheta_2)/\ Sin(\beta-\vartheta_1))$. For this profile, this ratio is about 2.6. which is in satisfactory agreement with the area ratio indicated by the change in U_n.

The results deduced for Flame #2 are shown in Table III. Compare to Flame #1, the equivalence ratio for this flame is higher, but with lower free-stream velocity. The incident turbulence intensities, owing largely to the additional fluctuations induced by the flame, are slightly higher. The parameter S_t / u' for the two flames are comparable and their turbulent burning velocities are not expected to be much different. However, the results show that the mean $S_t(\alpha)$ for Flame #2 is about 1.13 m/s which is much higher than $S_t(\alpha)$ = 0.29 m/s for Flame #1. The $S_t(\alpha)$'s of Flame #2 also vary from negative to positive with increasing x. On the other hand, the $S_t(\beta)$'s do not show a strong dependence on x, they average about 1.62m/s which is about the same as that obtained for Flame #1.

The results for Flame #5 are shown in Table IV. The main difference between this flame and Flame #1 is that the incident turbulence intensities are higher. Therefore, the turbulent burning velocities are expected to increase. The $S_t(\alpha)$'s for this flame are not much higher than those for Flame #1 though they do not show any dependence on x. At x=110 mm $S_t(\alpha)$'s for Flames #1 and #5 are about equal. It is of interest to note that the results based on the cold boundary (not shown) vary enormously from 0.4 m/s at x = 60.0 mm to 2.33 m/s at x = 110.0 mm. These results again emphasize the large discrepancy ~~in the results~~ due to the difference in the choice of flame surface. In contrast, the $S_t(\beta)$'s are much higher than those of Flame #1 and averaged about 2.4 m/s.

In Fig. 6 and 7, the turbulent burning velocity deduced for all our flames are shown on the S_t / S_u vs. S_u / u' plan. The $S_t(\alpha)$'s are shown in Fig. 6 and the $S_t(\beta)$'s are shown in Fig. 7. Also shown is the empirical correlation of Abdel-Gayed & Bradley [5]

for R_l of 100 to 150 corresponding to our experimental conditions. The arithmetic mean of the results obtained at $x \geq 70$ mm is plotted. The vertical bar indicates the range of S_t for each condition. The horizontal bar represents the variations in free-stream turbulence intensity. The $S_t(\alpha)$ results, Fig. 6, all fall below the correlation. Especially for Flame #4, #5 and #6, the deviations are quite substantial. Though it has been shown that the turbulent burning velocity for stabilized flames are generally lower than those observed in flame kernels, these deviations are too large to be meaningful. Moreover, quite a number of the data are lower than the laminar burning velocity. Whereas in Fig. 7, the $S_t(\beta)$ results are much more consistent with the correlation, and the scatter of the data is within the scatter of the data used by Abdel-Gayed & Bradley to deduce this correlation.

The $S_t(\alpha)$ results strongly suggest that the physical significance of the mean flame surface method needs to be examined. Regardless of which flame surface is used, this definition basically implies that the turbulent burning velocity is directly proportional to the flame angle, i.e. the inclination of the turbulent flame brush. Accordingly, an increase in free-stream turbulence should open up the v-flame thus increasing the flame angle. However, our schlieren observations show that this is not the major effect of the incident turbulence on the flame. The most apparent change is an increase in flame wrinkles which causes an increase in flame surface area [7]. The increase in burning velocity due to the increase in flame surface area is well known. This phenomenon is also shown in recent theoretical calculation by Ashurst and Barr [3] using the vortex dynamocs technique. Therefore, the change in flame angle is only a secondary effect as compare to the increase in flame wrinkling, as shown by the relatively small changes in α with increasing turbulence intensity (Tables II to IV). Consequently, definition of the turbulent burning velocity based solely on the change in flame angle does not seem to be sufficient to fully encapsulate all the effects of turbulence on flame propagation.

Another shortcoming of this method is that there is no standard for choosing the flame surface. In other flame configurations this may be irrelevant. But in this

configuration, it is quite crucial. Different investigators have used different flame surfaces which produced totally different results. This discrepancy is shown here again by the results based on the steepest gradient contour and on the cold boundary. Because of the large variation due to the choice of flame surface and also the variation of S_t from point to point, the results obtained by this method would be totally useless for comparing with other flames.

The second method we have proposed does not require a choice of flame surface, and is therefore less arbitrary than the flame surface method. Furthermore, the effective flame orientation is calculated from measured overall mean flow deflection, and can be associated with the most probable flame orientation which is a statistical property of the wrinkled flame sheet. These results compare much better with experimental correlations and do not show a strong dependence on the distance above the flame stabilizer. This method shows promise as a viable alternative for defining the turbulent burning velocity in this flame configuration, in view of the unsatisfactory results obtained by the first method. It can calso be implemented in other oblique flame configuration with the requirement that the flow velocity entering and leaving the flame brush are known.

One of the most important aspects of defining the turbulent bunding velocity is that the results would facilitate the development of numerical models of turbulent combustion. At present, one dimensional turbulent combustion model such as the one described in Bray et. al. [2] relies on emperical data of turbulent turbulent velocity as one of the input parameters. Although the v-shaped flame are highly two-dimensional, the results we have obtained can be transformed to the flame coordinate to be more consistent with the geometry of the model. On the other hand, two dimensional numerical model such as the one developed by Ashurst and Barr [3] using the vortex dynamic method is better-suited for predicting the turbulent velocity. As shown here, the results obtained by the mean flame surface are not very useful due to the inherent orbit of the method. The effective flame orientation method proposed here seems to be a logical choice for further exploration. Our current study of the v-shaped flame

using methane and propane will provide more S_t data based on this method for comparison with empirical correlations and numerical models.

SUMMARY

Our study of turbulent burning velocity in six premixed ethylene/air v-shaped flame has shown that the results obtained close to the flame stabilizer is meaningless. This is due to the fact that the flame propagation in this region is dominated by the flame stabilizer wake. The results obtained above this wake region show variations along the flame brush. This shows that the study of turbulent burning velocity should not be confined to only one location on the flame brush.

The use of conventional flame surface method for deducing S_t is not at all satisfactory. One of the major reasons is that the results depend on the choice of the flame surface. Moreover, it is found that the variation of S_t along the flame can be several times the laminar burning velocity. Due to the large scatter, it does not seem meaningful to deduce a typical representative mean S_t. The arithmetic average of the results based on the steepest gradient contour are calculated for the purpose of comparison. They are generally lower than those observed in flame kernels under similar turbulent conditions, with some data falling below the laminar burning velocity. More importantly, they do not clearly show an increase with increase incident turbulence, contradicting the principle of turbulent flame propagation.

The results based on an effective flame orientation, deduced from mean flow deflection, compare much better with empirical correlation. The effective flame orientation is shown to be associated with the statistical propertes of the orientation of the wrinkled turbulent flame sheet. This method seem to be a viable alternative to the conventional flame surface method and is less arbitary because the results do not depend on the choice of the flame surface.

Also, our study clearly demonstrate the need to develope a consistent method of deducing the turbulent burning velocity in oblique turbulent flames so that the results would be more useful to the understanding of turbulent flame propagation and for

comparison with theoretical calculations.

ACKNOWLEDGEMENT

The authors are most grateful to Prof. Felix Weinberg for his valuable discussions and suggestions. The authors would also like to thank Dr. F. Robben and Prof. L. Talbot for their continued advice and support.

This work was supported by the Director, Office of Energy Research, Office of Basic Energy Sciences, Chemical Sciences Division of the U. S. Department of Energy under Contract No. DE-AC-03-76SF00098.

REFERENCES

[1] Bray, K. N. C., and Libby P. A., *Physics of Fluids*, *19*, 11, 687, (1979).

[2] Bray, K. N. C., Libby, P. A., Masuya, Goro, and Moss, J. B., *Combustion Science and Technology*, *25*, 127, (1981).

[3] Ashurst, W. T., Barr, P. K., "Stochastic Calculation of Laminar Wrinkled Flame Propagation via Vortex Dynamics," to appear in *Combustion Science and Technology* , (1983).

[4] Ballal, D. R., and Lefebvre, A. H., *Proc. R. Soc. Lond.*, A 344, 217 (1975).

[5] Abdel-Gayed, R. G., and Bradley, D., *Sixteenth Symposium (International) on Combustion*, The Combustion Institute, 1752 (1977).

[6] Cheng, R. K., and Ng, T. T., *First Specialist Meeting (International) of the Combustion Institute*, The French Section of the Combustion Institute, *1*, 13, (1981).

[7] Cheng, R. K., and Ng, T. T., *Combustion and Flame*, *52*, 185, (1983).

[8] Namazian, M., Talbot, L., Robben, F. and Cheng, R. K., *Nineteenth Symposium (International) on Combustion*, The Combustion Institute, 487 (1982).

[9] Ho, C. M., Jakus, K., and Parker, K. H., *Combustion and Flame*, *27*, 1, 113 (1976).

[10] Smith, K. O. and Gouldin, F. C., *AIAA J., vol 17*, 11, 1243 (1979).

[11] Dandekar, K. V. and Gouldin, F. C., *AIAA J., vol 20*, 5, p. 652, (1982).

[12] Bill, R. G., Jr., Namer, I., Talbot, L., Cheng, R. K., and Robben, F., *Combustion and Flame*, *43*, 3, 229 (1981).

[13] Cheng, R. K., Popovich, M. M., Robben, F., and Weinberg, F. J., *J. Phys. E: Sci. Instrum.*, *13*, 315, (1980).

[14] Peterson, R. E., and Emmons, H. W., *Phys. of Fluids*, *4*, 456, (1961).

[15] Suzuki, T., Hirano, T., and Tsuji, H., *Seventeenth Symposium (International) on Combustion*, 289, (1978).

[16] Raezer, S. D., and Olsen H. L. *Combustion and Flame*, *6*, 227, (1962).

[16] Kleine, R. "Anwendung der Laser-Doppler-Anemometrie zur Bestimmung der turbulenten Flammengschwinidigkeit," Thesis Karlshure (1974).

[17] Gunther, R., *Progress in Energy and Combustion Science*, *9*, 105, (1983).

Table 1 Experimental Conditions

Flame no.	U_∞ (m/s)	ϕ	Turbulence Generator	Free-stream turbulence at x=60mm u'/U_∞(%)	v'/U_∞(%)	l_x mm
1	7.0	0.75	grid	5.0	5.0	5.0
2	5.0	0.8	grid	6.0	6.0	4.5
3	5.0	0.7	grid	4.5	4.5	5.0
4	7.0	0.66	grid	5.0	5.0	5.0
5	7.0	0.75	plate #1	7.0	5.5	4.0
6	7.0	0.75	plate #2	8.5	7.6	3.5

Turbulence Generator	Description	Blockage Factor
Grid	5.0mm square mesh with 1.0mm elements	36%
Perforated Plate #1	3.2mm circular holes, 1.6mm apart	60%
Perforated Plate #2	4.7mm circular holes, 1.8mm apart	52%

Table II Comparison of turbulent burning velocity based on the steepest gradient contour, $S_t(\alpha)$, and the effective flame orientation $S_t(\beta)$, for Flame #1.

x(mm)	S_u/u'	α	$S_t(\alpha)$ m/s	$S_t(\alpha)/S_u$	β	$S_t(\beta)$ m/s	$S_t(\beta)/S_u$
60.0	2.4	10.2	-0.43				
70.0	2.4	11.4	0.20	0.42	24.5	1.63	3.4
80.0	2.0	12.6	0.11	0.23	29.4	1.96	4.0
90.0	1.7	13.9	0.24	0.49	23.3	1.34	2.8
100.0	1.7	15.1	0.35	0.73	25.2	1.57	3.3
110.0	1.6	16.2	0.58	1.20	25.8	1.75	3.6

Table IIb Turbulent burning velocity for Flame #1 based on the cold boundary

x(mm)	S_u/u'	α_{cb}	S_t m/s	S_t/S_u
70.0	2.4	14.0	0.37	0.77
80.0	2.4	16.7	0.79	1.65
90.0	2.0	19.3	1.01	2.10
100.0	1.7	20.8	1.20	2.50
110.0	1.6	21.8	1.35	2.8

Table III Comparison of turbulent burning velocity based on the steepest gradient contour, $S_t(\alpha)$, and the effective flame orientation $S_t(\beta)$, for Flame #2.

x(mm)	S_u/u'	α	$S_t(\alpha)$ m/s	$S_t(\alpha)/S_u$	β	$S_t(\beta)$ m/s	$S_t(\beta)/S_u$
60.0		9.8	-0.63				
70.0	1.7	23.3	0.4	0.80			
75.0	1.52	29.1	1.18	2.36	34.0	1.66	3.32
80.0	1.43	34.4	1.35	2.70	36.4	1.52	3.04
85.0	1.7	39.1	1.58	3.16	40.4	1.69	3.38

Table IV Comparison of turbulent burning vleocity based on the steepest gradient contour, $S_t(\alpha)$, and the effective flame orientation $S_t(\beta)$, for Flame #5.

x(mm)	S_u/u'	α	$S_t(\alpha)$ m/s	$S_t(\alpha)/S_u$	β	$S_t(\beta)$ m/s	$S_t(\beta)/S_u$
60.0		15.0	0.8	1.67			
70.0	1.04	17.0	0.6	1.24			
80.0	0.96	18.0	0.56	1.16	33.8	2.5	5.21
90.0	1.04	20.8	0.6	1.25	35.6	2.09	4.35
100.0	1.0	22.6	0.57	1.18	38.6	2.59	5.39

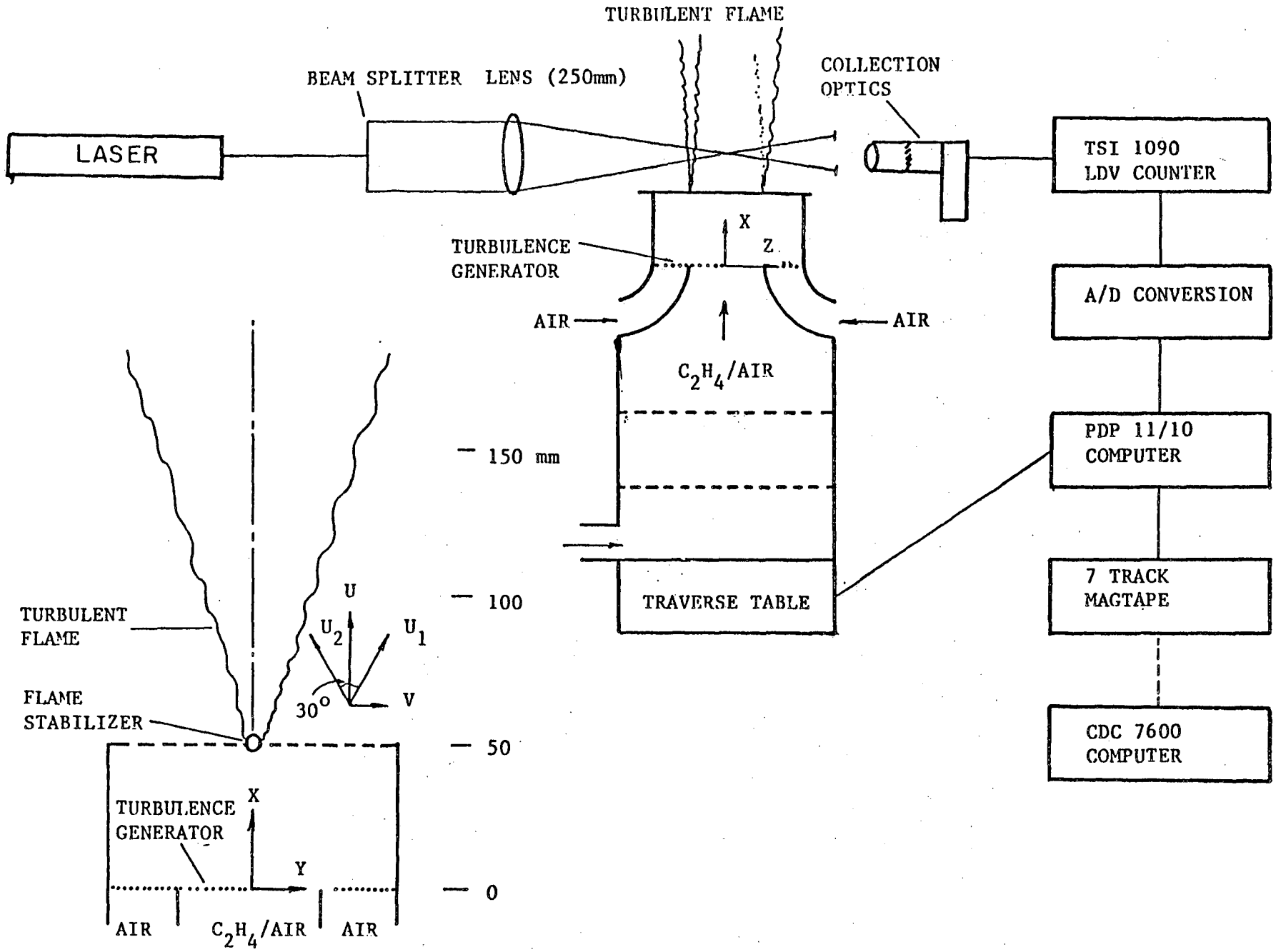

Fig. 1 Schematics of the experimental setup and the data acquisition system.

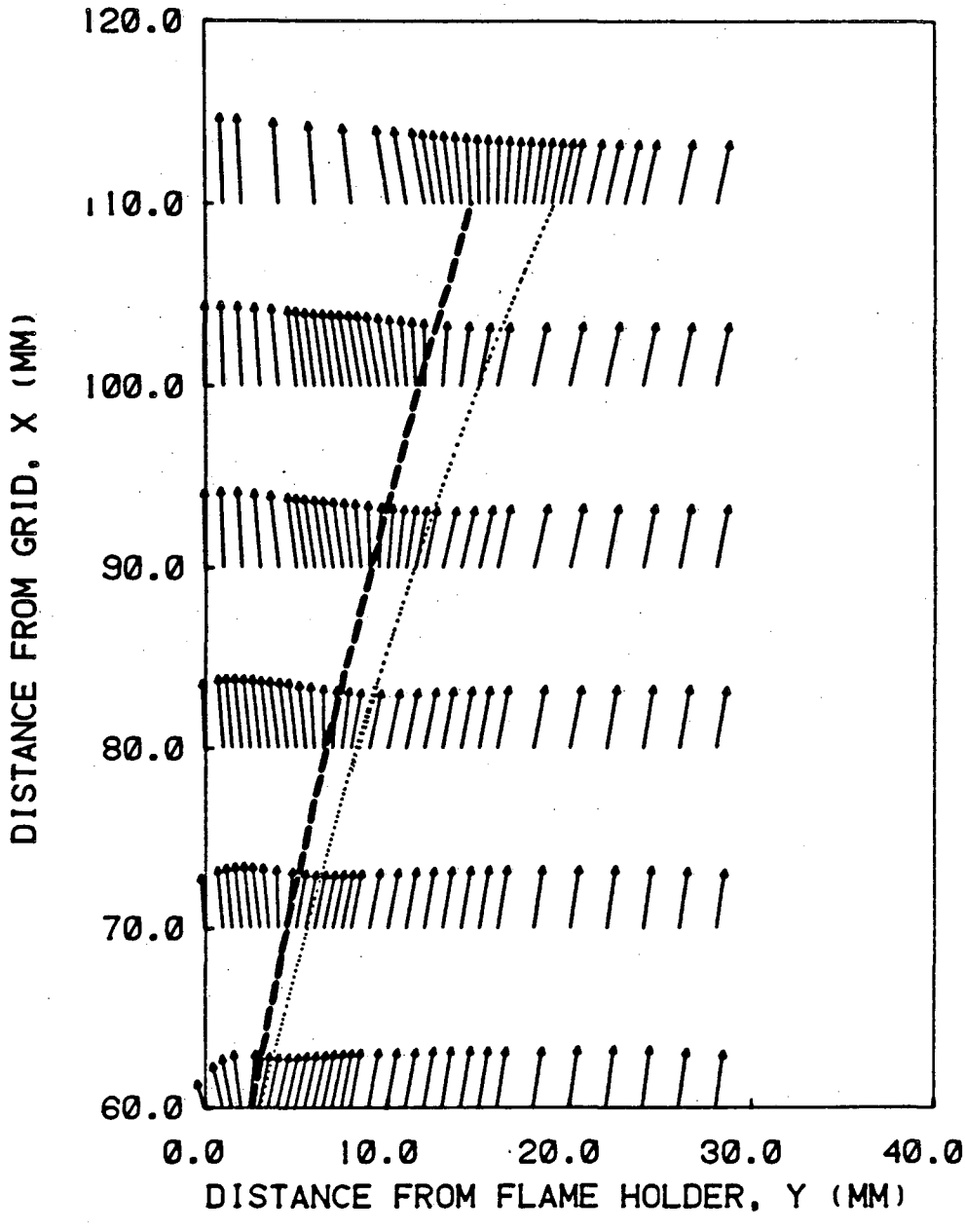

Fig. 2 Velocity vectors in the flow-field of Flame #1, ---- time-mean flame surface, ... cold boundary.

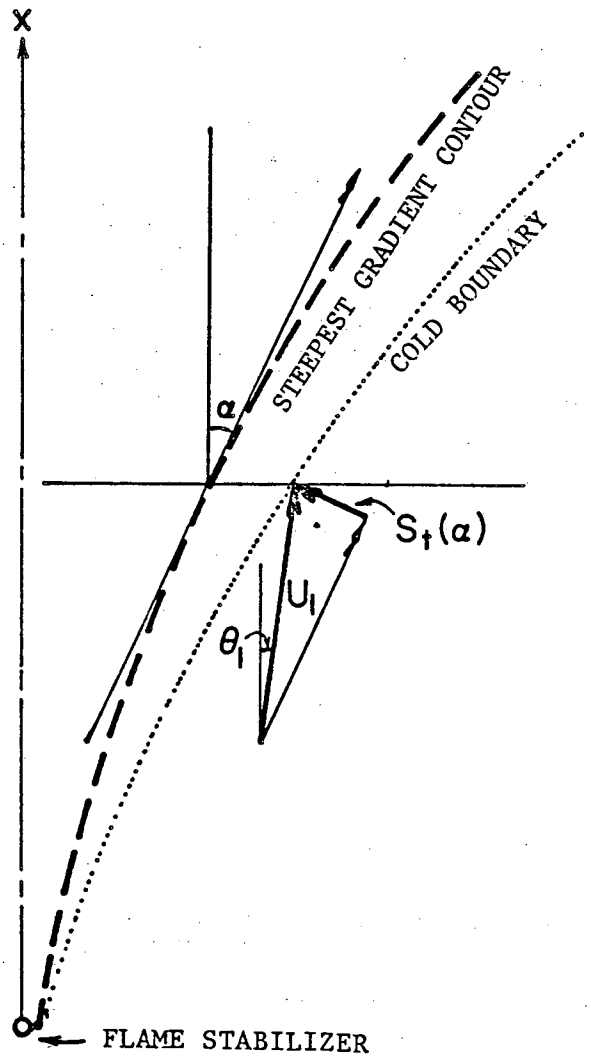

Fig. 3 Definition of $S_t(\alpha)$ based on the steepest gradient contour.

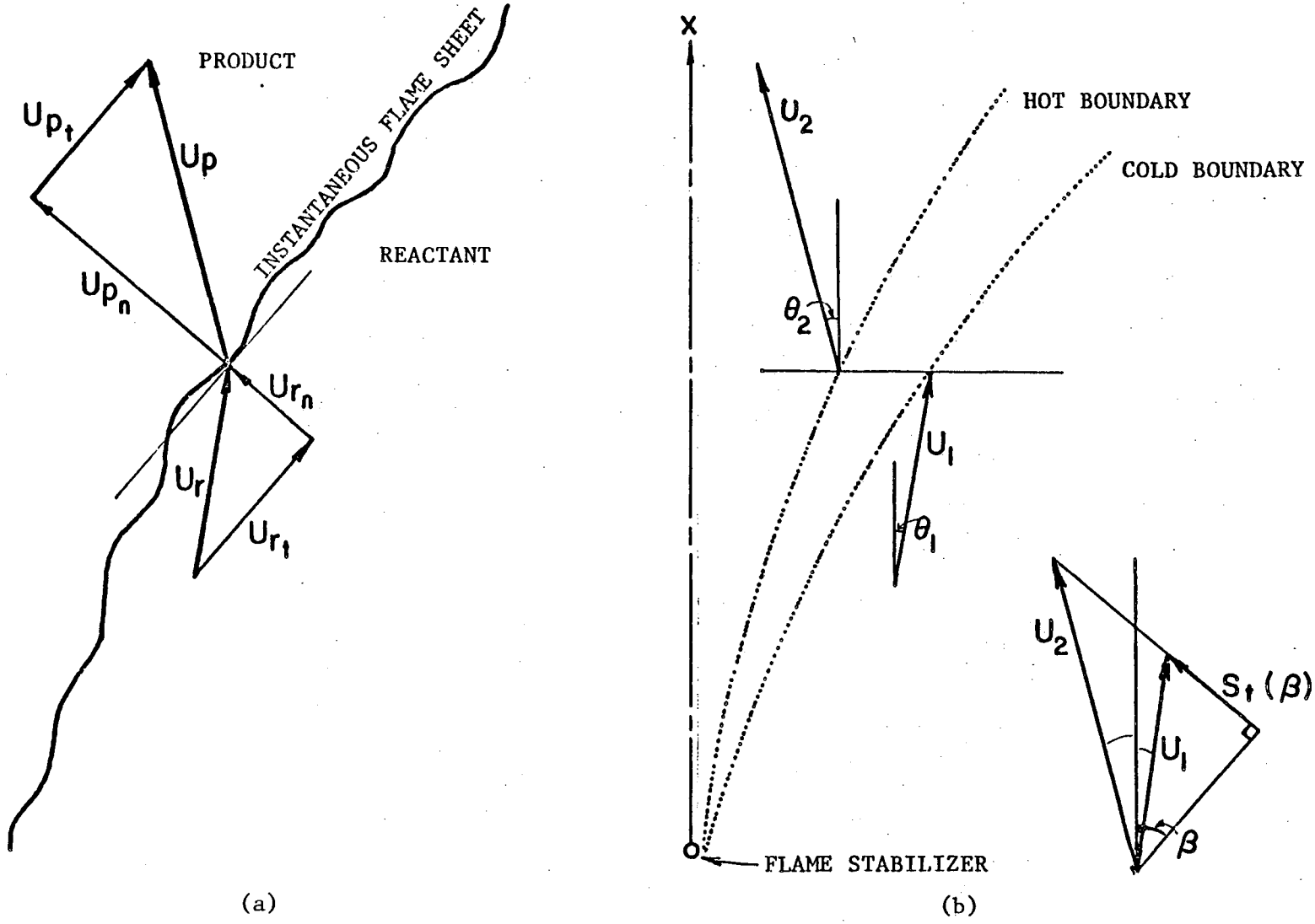

Fig. 4 (a) interaction of the flow with the instantaneous flame sheet, (b) definition of $S_t(\beta)$ based on the effective flame orientation.

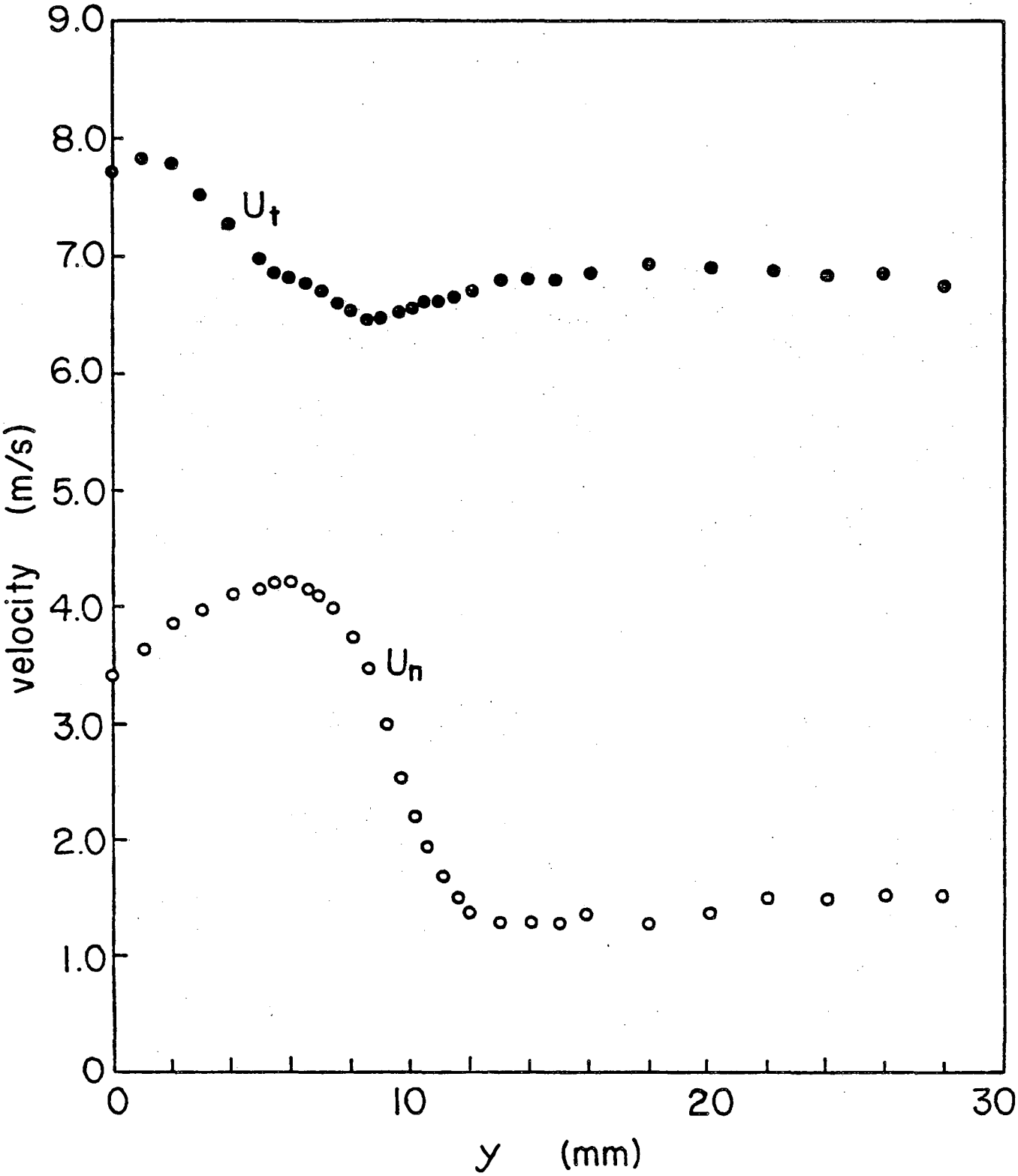

Fig. 5 Profiles of velocity tangential, U_t and normal, U_n, to the effective flame orientation of Flame #1 at x^t= 90 mm.

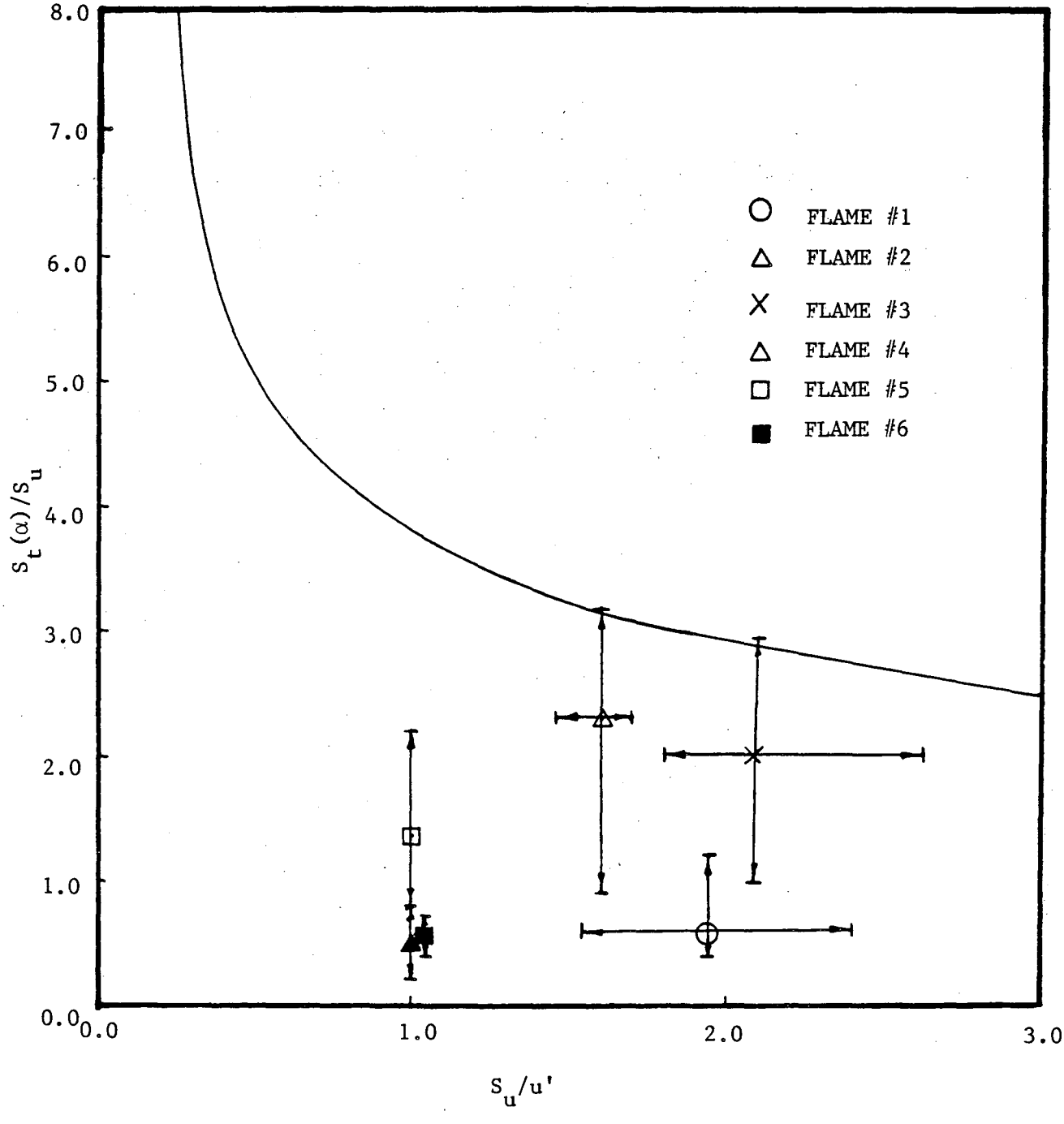

Fig. 6 Comparison of $S_t(\alpha)$ with correlation of Abdel-Gayed and Bradley for R_l = 100 to 150.

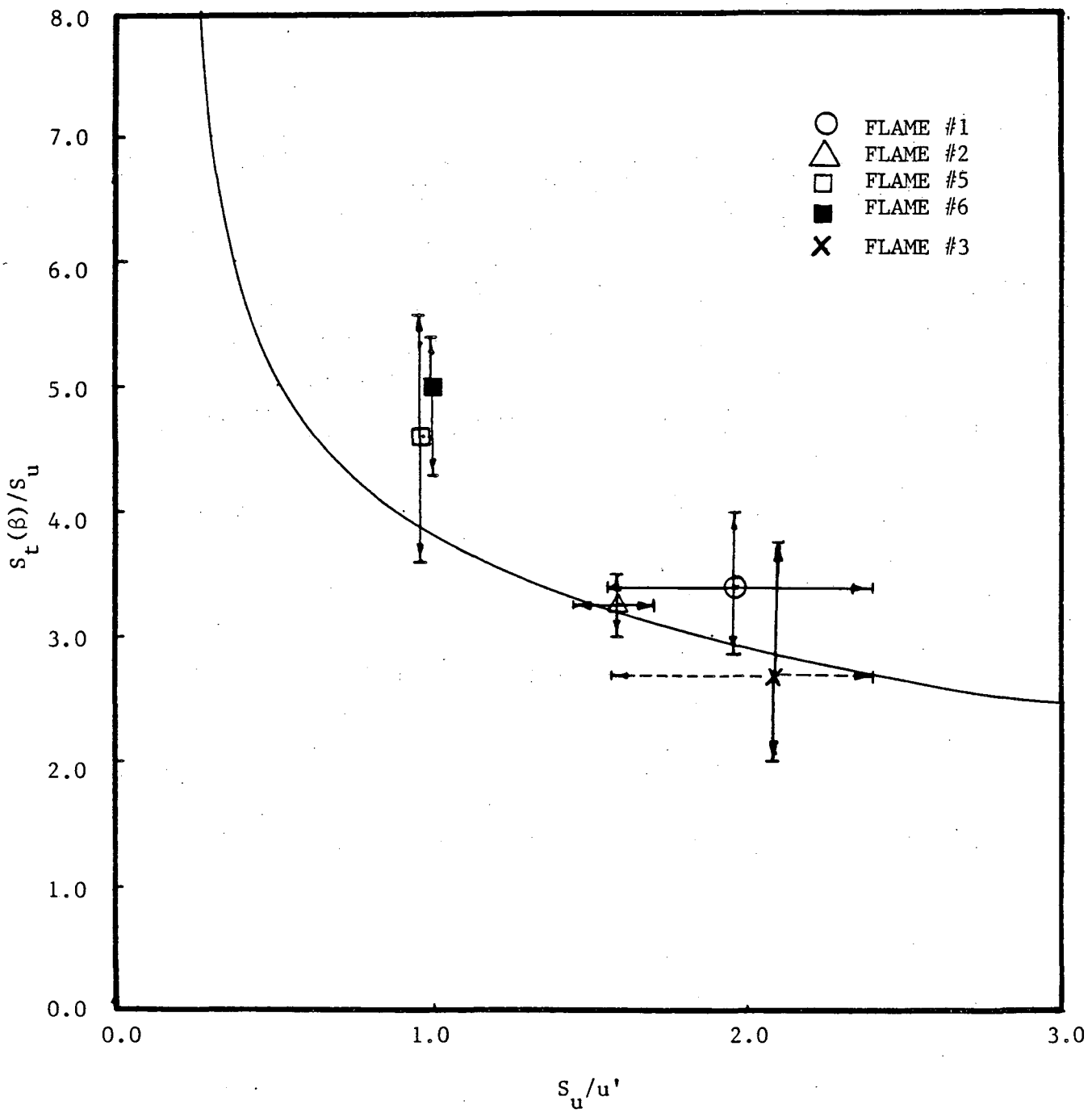

Fig. 7 Comparison of $S_t(\beta)$ with correlation of Abdel-Gayed and Bradley for R_l = 100 to 150.

TECHNICAL INFORMATION DEPARTMENT
LAWRENCE BERKELEY LABORATORY
UNIVERSITY OF CALIFORNIA
BERKELEY, CALIFORNIA 94720